# A Shape Memory Alloy Model for Uranium-Niobium Accounting for Plasticity

SANJAY GOVINDJEE* AND ERIC P. KASPER
*Department of Civil Engineering, University of California, Berkeley, CA 94720*

**ABSTRACT:** In this paper we present a 1-D model for the behavior of U-Nb shape memory alloys that accounts for the effect of plastic deformations on recovery strains. In particular, we account for the erasure of memory effect that occurs with increasing plastic strains. An algorithmic approximation to the model is discussed in detail and a comparison to some experimental results is shown.

## INTRODUCTION

URANIUM-NIOBIUM alloys with roughly 13% Nb to 18% Nb display a shape memory effect. At high temperatures these alloys are in the $\gamma$ phase which has a bcc type structure—austenitic phase. As the temperature is lowered the material passes through the $\gamma^o$ phase with a tetragonal structure, the $\alpha''$ phase with a monoclinic structure, and finally to an $\alpha'$ phase with an orthorhombic structure. Typical phase diagrams show $\alpha''$ and $\gamma^o$ as the stable low temperature phases (martensitic phases) though this is a strong function of composition; see, e.g., Vandermeer et al. (1981).

The basic kinetics of the material phase transformations appear to follow along the lines of classical shape memory alloys at moderate stress levels; see Funakubo (1984) for further details. An important consideration, however, in using such materials is that they are often plastically deformed and thus the effects of plasticity must be accounted for in any model that purports to mimic their complex behavior. As a stepping stone to building a model capable of this, we propose here a simple 1-D model that has the flexibility to incorporate the effects of plasticity and be computationally robust and efficient. The model in many respects can be considered an extension and simplification of the model of Brinson and Lammering (1993) and Tanaka (1986).

## CONSTITUTIVE EQUATION

A constitutive model for a U-Nb alloy needs to model shape memory effects and plasticity and their interaction. In the model presented below, we restrict ourselves to the shape memory phase transformations of multi-variant de-twinning of martensite, austenite production from martensite, and multi-variant martensite production from austenite. For simplicity, we ignore the production of single variant martensite from austenite. The inclusion of this added transformation formally presents no difficulties; it was merely not needed for the experimental data examined.

The plasticity model accounts for behavior at high stresses and is assumed to govern the behavior when no other transformations are occurring similar to Ford and White (1996). Thus it is most well suited to plasticity at temperatures below the martensite start temperature. The plasticity model is not designed for use with plasticity occurring at high temperatures where phase transformations are possibly occurring. Note that adequate experimental data does not exist in this regime of behavior making realistic modeling all but impossible. Nor is it suited to materials where the critical finish stress for the de-twinning process is above the yield stress—a situation that likely does not occur in nature.

The coupling between the plasticity and shape memory effects of the model centers around the influence of plastic strain on the kinetics of the martensite to austenite phase transformation. It is this phase transformation that is central to the shape memory effect (SME). In the SME one is interested in the recovery of large strains that have been mechanically induced. The strains are related to the generation of single variant martensite from multi-variant martensite. The SME comes about from the reverse process that can only occur by first creating austenite and then converting the austenite into multi-variant martensite. When plasticity occurs the motion and generation of dislocations interferes with this process [Vandermeer et al. (1981), Jing-Chen et al. (1990), and Dutkiewicz (1994)] and we encounter an apparent erasure of memory in the material. The amount of memory lost is a function of the plastic strain in the material. The mechanistic picture of how at high stress the motion and generation of dislocations in the material interferes with the phase transformation process is not well understood. Possible explanations, for example, include the presence of internal stress fields that "lock-in" single-variant martensite structures or possibly the destruction of the martensite symmetry through excessive defect populations. Whatever the true explanation, one is left

*Author to whom correspondence should be addressed.



1045-389X/97/10 0815-09 $10.00/0

with a situation where the stress induced single variant martensite phase does not fully transform to austenite upon the "usual" heating cycle. Without the conversion of the single-variant martensite into austenite, the reversion to a twinned multi-variant phase is impossible. Thus the material effectively loses its memory. The simple model presented below is devoted to incorporating these effects in as simple a fashion as possible and yet remain faithful to the basics of the available experimental data on U-Nb alloys.

### Stress-Strain

Our fundamental hypothesis is that the 1-D stress-strain relation may be written as

$$\sigma = E[\varepsilon - \varepsilon^p - \varepsilon_L(\xi^+ - \xi^-) - \alpha\Delta T] \qquad (1)$$

where $\sigma$ is the stress, $E$ is the elastic modulus, $\varepsilon$ is the total strain, $\varepsilon^p$ is the plastic strain, $\varepsilon_L$ is the maximum residual strain obtained by de-twinning multiple variant martensite (Bain or transformation strain), $\xi^+$ and $\xi^-$ are the volume fractions of the positive and negative variants of the martensite twins [Achenbach et al. (1986) or Pence et al. (1994)], $\alpha$ is the coefficient of thermal expansion and $\Delta T$ is the change in the temperature field from a reference temperature. Note that for simplicity we assume only a two variant martensite. For a more complete model one should account for all possible variants [see Boyd and Lagoudas (1996a,b)].

*REMARK 1:* In some models a linear mixture rule for the elastic material modulus $E = E_a + \xi(E_m - E_a)$ is used, where $E_a$ and $E_m$ are the elastic moduli for pure austenite and martensite, respectively. If so desired, one can modify this rule of mixtures to also include a change in modulus for de-twinned martensite from multi-variant martensite. For the present demonstration, however, we will assume the modulus to be a constant. (Note that the total martensite fraction is simply the sum of the variants; $\xi = \xi^+ + \xi^-$.)

The key to completing the specification of the model is the construction of a set of evolution rules for the internal variables: plastic strain, equivalent plastic strain, and the martensite fractions. This point is addressed in the next section.

## EVOLUTION EQUATIONS

### Plasticity

For the plasticity we assume a simple linear isotropic hardening model. The basic internal variables are the plastic strain and the equivalent plastic strain. The governing flow rules are:

$$\dot{\varepsilon}^p = \lambda \ \text{sign}\ [\sigma] \qquad (2)$$

$$\dot{\bar{\varepsilon}}^p = \lambda \qquad (3)$$

with the yield function

$$\phi(\sigma, \bar{\varepsilon}^p) = |\sigma| - (\sigma_y + H\bar{\varepsilon}^p) \qquad (4)$$

and Kuhn-Tucker conditions

$$\phi \le 0; \quad \lambda \ge 0; \quad \lambda\phi = 0; \quad \lambda\dot{\phi} = 0 \qquad (5)$$

*PLASTICITY ALGORITHM*

Algorithmically, we treat these equations using a closest-point projection method [Simo and Hughes (1998)]—which amounts to a radial return algorithm in the present situation. A synopsis of this well known algorithmic procedure is given in Table 1 for the advancement of a known state of time $t_n$ to a new state at time $t_{n+1}$ when the total strain increment is known.

*REMARK 2:* Note that the internal variables for the martensite are considered constants by assumption when plasticity is active; i.e., $\xi^+_{n+1} = \xi^+_n$ and $\xi^-_{n+1} = \xi^-_n$. Further, we assume here and throughout that the temperature time history is known as far as the mechanical problem is concerned.

### Production of Single Variant Martensite

The evolution of the positive variant of the martensite fraction may be expressed in its integrated form as a linear interpolation within the phase transition region shown in Figure 1:

**Table 1.**

1. Define trial state $\sigma^{tr} = \sigma_n + E[\Delta\varepsilon - \alpha\Delta T]$, $\varepsilon^{p(tr)} = \varepsilon^p_n$, $\bar{\varepsilon}^{p(tr)} = \bar{\varepsilon}^p_n$

2. If $\phi(\sigma^{tr}, \bar{\varepsilon}^{p(tr)}) \le 0$, then elastic step

$$\sigma_{n+1} = \sigma^{tr} \qquad (6)$$

$$\varepsilon^p_{n+1} = \varepsilon^p_n \qquad (7)$$

$$\bar{\varepsilon}^p_{n+1} = \bar{\varepsilon}^p_n \qquad (8)$$

Go to step 4.

3. If $\phi(\sigma^{tr}, \bar{\varepsilon}^{p(tr)}) > 0$, then return map

$$\Delta\lambda = \phi^{tr}/(E + H) \qquad (9)$$

$$\sigma_{n+1} = \sigma^{tr} - \Delta\lambda E \ \text{sign}\ [\sigma^{tr}] \qquad (10)$$

$$\varepsilon^p_{n+1} = \varepsilon^p_n - \Delta\lambda \ \text{sign}\ [\sigma^{tr}] \qquad (11)$$

$$\bar{\varepsilon}^p_{n+1} = \bar{\varepsilon}^p_n + \Delta\lambda \qquad (12)$$

4. Compute consistent tangent: If elastic $E$, else $EH/(E + H)$.

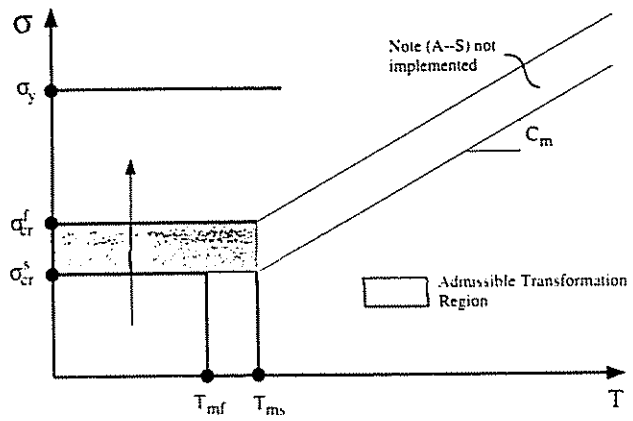


*Figure 1. Production of single variant martensite from a low temperature state.*

$$\xi^+ = 1 + (1 - \xi_0^+)\frac{(\sigma - V_{mf})}{(V_{mf} - V_{ms})} \tag{13}$$

The parameters $V_{ms}$ and $V_{mf}$ denote critical values of stress between which the martensitic transformation occurs, where the subscripts *ms* and *mf* designate the martensite start and finish values, respectively. The actual starting value of the transformation is taken to be a function of the initial fractions present when the transformation process begins $(\xi_0^+, \xi_0^-)$, while the finish value is taken to be constant:

$$V_{ms} = \sigma^s_{cr} + (\xi_0^+ - \xi_0^-)(\sigma^f_{cr} - \sigma^s_{cr}), \quad V_{mf} = \sigma^f_{cr} \tag{14}$$

The evolution of the negative variant may be readily obtained as a consequence of the positive variant production

$$\xi^- = \xi_0^- \frac{(1 - \xi^+)}{(1 - \xi_0^+)} \tag{15}$$

while the total fraction martensite fraction remains constant at

$$\xi = \xi^+ + \xi^- = 1 \tag{16}$$

during this process.

*REMARK 3:* If the total martensite fraction is not unity during this phase transformation, special forms of Equations (13) and (15) need to be used:

$$\xi^+ = \xi_0 + (1 - \xi_0^+)\frac{(\sigma - V_{mf})}{(V_{mf} - V_{ms})} \tag{17}$$

$$\xi^- = \xi_0^- \frac{(\xi_0 - \xi^+)}{(\xi_0 - \xi_0^+)} \tag{18}$$

In what follows we will not treat this case.

*SINGLE VARIANT PRODUCTION ALGORITHM*

Algorithmically, this transformation is treated via a trial state approach. One first computes $\sigma^{tr} = \sigma_n + E[\Delta\varepsilon - \alpha\Delta T]$. If,

$$\sigma^{tr} > V_{ms} \tag{19}$$

$$T < T_{ms} \tag{20}$$

$$\xi_n^+ < 1 \tag{21}$$

and

$$\sigma^{tr} > \sigma_n \tag{22}$$

then one is presumed to be transforming multiple variant martensite into single variant martensite. Once a transformation has been detected, the martensite fractions and the stress are determined by simultaneously solving the linear Equations (13), (15) and (1) for the martensite fractions and the stress. Note that the initial fractions $\xi_0^{(\cdot)}$ are history variables that are set at the martensite fractions at the first time a transformation region becomes active. These values persist as $\xi_0^{(\cdot)}$ until the material becomes elastic again at which time they are reset. This procedure is effective for the handling of internal loops within transformation regions.

*REMARKS 4:* When using such models in an engineering analysis program such as a finite element code one typically also needs to know the algorithmic tangent of the stress-strain model. During this transformation process it is given by

$$E^{algo} = \frac{E}{1 + E\varepsilon_L\left(\dfrac{1 - \xi_0^+ + \xi_0^-}{V_{mf} - V_{ms}}\right)} \tag{23}$$

**Production of Multiple Variant Martensite**

The evolution of the total martensite fraction may be expressed in its integrated form as a linear interpolation within the phase transition region shown in Figure 2:

$$\xi = 1 + (1 - \xi_0)\frac{(T - \theta_{mf})}{(\theta_{mf} - \theta_{ms})} \tag{24}$$

The parameters $\theta_{ms}$ and $\theta_{mf}$ denote critical values of temperature between which the martensite transformation occurs, where the subscripts *ms* and *mf* designate the martensite start and finish values, respectively. The starting value of the transformation is taken to be a function of the initial

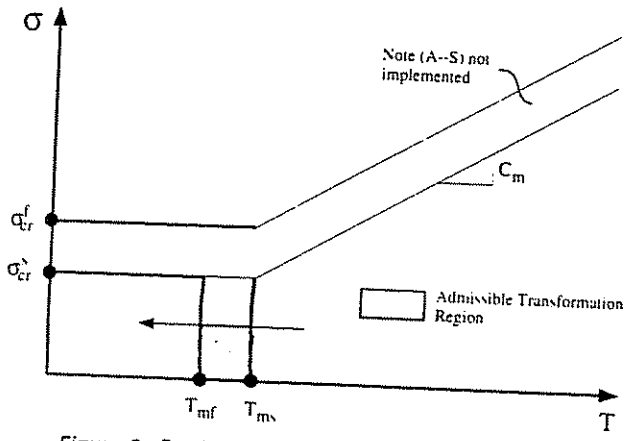


*Figure 2. Production of multiple variant martensite.*

fractions present, while the finish value is taken to be constant

$$\theta_{ms} = T_{ms} + \xi_0 (T_{mf} - T_{ms}), \quad \theta_{mf} = T_{mf} \tag{25}$$

The evolution of the positive and negative variants are obtained by assuming random (equal) production of the plus and minus martensite variants:

$$\xi^+ = \xi_0^+ + \frac{1}{2}(\xi - \xi_0), \quad \xi^- = \xi_0^- + \frac{1}{2}(\xi - \xi_0) \tag{26}$$

*MULTIPLE VARIANT PRODUCTION ALGORITHM*

Algorithmically, this transformation is also treated via a trial state approach. One first computes $\sigma^{tr} = \sigma_n + E[\Delta\varepsilon - \alpha\Delta T]$. If,

$$\sigma^{tr} < Y_{ms} \tag{27}$$

$$T < T_{ms} \tag{28}$$

$$\xi_n < 1 \tag{29}$$

and

$$T_{n+1} < T_n \tag{30}$$

then one is presumed to be transforming austenite into multiple variant martensite. Once a transformation has been detected, the martensite fractions are updated according to Equations (24) and (26) and the stress is updated using Equation (1).

*REMARK 5:* The algorithmic tangent during this transformation process is given by

$$E^{algo} = E \tag{31}$$

**Production of Austenite**

In the production of austenite from martensite one needs to consider the effects of plastic deformations. When the materials in the de-twinned (single variant) phase are deformed plastically, the single variant martensitic structure begins to loose its ability to transform into austenite. To model this effect, we consider a modification of the usual evolution laws during this transformation to account for equivalent plastic strains. The evolution of the total martensite fraction may be expressed in its integrated form as a linear interpolation within the phase transition region shown in Figure 3:

$$\xi = \xi_0 + \left(1 - f(\bar{\varepsilon}^p) - \xi_0\right) \frac{(\sigma - Y_{as})}{(Y_{af} - Y_{as})} \tag{32}$$

In Equation (32), $f(\bar{\varepsilon}^p)$ can be interpreted the maximum amount of austenite that can be produced for a given amount of equivalent plastic strain.

*REMARK 6:* In the example shown later, we will assume the following two parameter functional form:

$$f(\bar{\varepsilon}^p) = (1 - \delta)\exp[-k\bar{\varepsilon}^p] + \delta \tag{33}$$

thus when there is no plastic strain the material is free to produce 100% austenite during this phase transformation. For finite values of $\bar{\varepsilon}^p$, the maximum amount of producible austenite is limited to a value between unity and the asymptotic value of $\delta$, taken as a material constant. The rate at which this asymptotic value is approached depends on the material parameter $k$.

The parameters $Y_{as}$ and $Y_{af}$ denote critical values of stress between which the transformation occurs, where the subscripts *as* and *af* designate stress values on modified (by initial fraction) austenite start and finish lines, respectively. The starting value of the transformation is taken to be a function

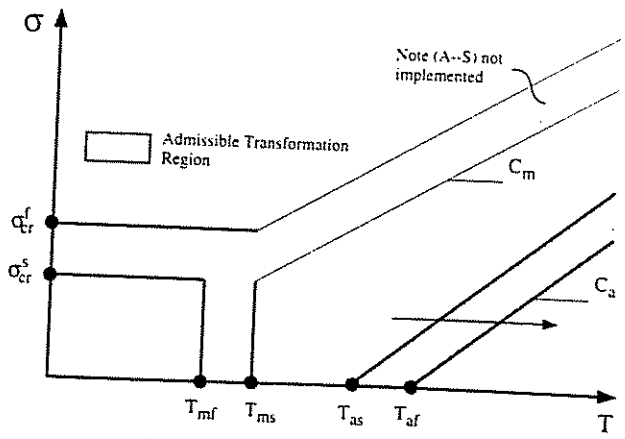


*Figure 3. Production of austenite.*

of the initial fractions present, while the finish value is taken to be constant; thus,

$$V_{as} = \sigma_{as} + (1-\xi_0)(\sigma_{af} - \sigma_{as}), \quad V_{af} = \sigma_{af} \quad (34)$$

where $\sigma_{as}$ and $\sigma_{af}$ are defined from the virgin transformation lines in stress-temperature space as

$$\sigma_{as} = C_a(T - T_{as}) \text{ and } \sigma_{af} = C_a(T - T_{af})$$

where $C_a$ is the slope of the transformation lines. The evolution of the positive and negative variants are assumed to occur in proportion to their existence at the beginning of the phase transformation; i.e.,

$$\xi^+ = \frac{\xi_0^+}{\xi_0}\xi \text{ and } \xi^- = \frac{\xi_0^-}{\xi_0}\xi \quad (35)$$

*MULTILINEAR PRODUCTION OF AUSTENITE*

The evolution model of the phase fractions described above is linear. In order to more accurately capture experimental data a non-linear evolution is more appropriate. From the standpoint of numerical computations many of the proposed nonlinear evolution equations pose difficult root finding problems where multiple admissible roots are available. As a simple, robust, and effective way of approximately incorporating arbitrary evolution paths we can assume a general piecewise linear form for the production of austenite. The description given below is also applicable to the de-twinning transformation and multiple variant production transformation through minor changes in terminology. For the data available, however, it is currently only justifiable for the production of austenite. We begin by redefining Equation (32) as

$$\xi = \xi_i + (\xi_{i+1} - \xi_i)\frac{(\sigma - V_i)}{(V_{i+1} - V_i)} \quad (36)$$

where both $\xi_i$ and $V_i$ are derived from user defined constitutive parameters. These parameters are depicted in Figure 4 which shows the austenite ($\xi_A = 1-\xi$) production curve as a function of temperature at constant stress.

The user defined parameters are the breakpoints in the multilinear approximation to the curve. Thus the $\gamma_i$'s determine the percentage of the total transformation that has occurred at the values of the $\beta_i$'s, which correspond to percent "distance" into the transformation temperature range. Explicitly, this yields the following relation for $\xi_i$:

$$\xi_i = \xi_0 - \gamma_i[\xi_0 - (1-f)] \quad \gamma_i \in [0,1]$$

$$\gamma_0 \le \gamma_1 \le \cdots \le \gamma_{n-1} \le \gamma_n$$

$$\text{where } \gamma_0 = 0 \text{ and } \gamma_n = 1$$

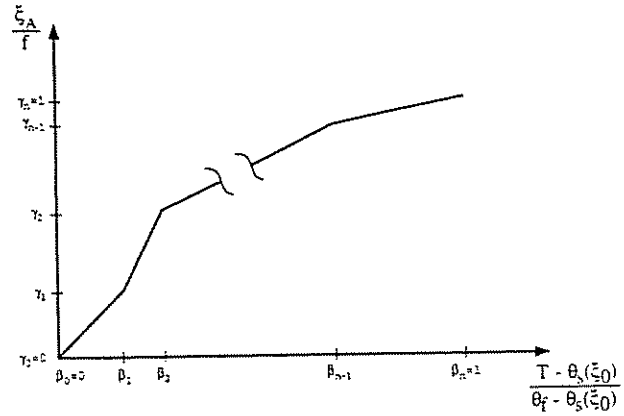


*Figure 4. Production of austenite curve definition at constant stress.*

and the following relation for $V_i$:

$$V_i = V_{as} - \beta_i[V_{as} - V_{af}] \quad \beta_i \in [0,1]$$

$$\beta_0 \le \beta_1 \le \cdots \le \beta_{n-1} \le \beta_n$$

$$\text{where } \beta_0 = 0 \text{ and } \beta_n = 1$$

*AUSTENITE PRODUCTION ALGORITHM*

Like the other transformations, this transformation is treated via a trial state approach. One first computes $\sigma^{tr} = \sigma_n + E[\Delta\varepsilon - \alpha\Delta T]$. If,

$$T > T_{as} \quad (37)$$

$$\sigma^{tr} < V_{as} \quad (38)$$

$$\xi_n > 1 - f(\bar{\varepsilon}^p) \quad (39)$$

$$\sigma^{tr} - \sigma_n < C_a(T_{n+1} - T_n) \quad (40)$$

and

$$T_{n+1} > T_n \quad (41)$$

then one is presumed to be transforming martensite into austenite. Once a transformation has been detected, the martensite fractions and stress are determined by simultaneously solving the linear Equations (32) or (36), (35), and (1). When using the multilinear transformation curve, one must algorithmically determine the "branch" or "branches" of the multilinear curve that are active. This can be efficiently done by simply starting with the branch $k$ for which $\xi_{k-1} < \xi_n < \xi_k$ and using Equation (36) with $i = k$ when solving for the martensite fraction. If the computed value of the martensite fraction is less than $\xi_{k-1}$, then re-solve for the martensite fractions using Equation (36) with $i = k + 1$, etc. This process stops when the computed value of $\xi$ lies within

the active branch or it is computed to be less than $\xi_n = 1 - f$ in which case it is set to $1 - f$.

*REMARK 7:* The consistent algorithmic tangent during this transformation process is given by

$$E^{algo} = \frac{E}{1 + E\varepsilon_L \dfrac{\xi_0^+ - \xi_0^-}{\xi_0} \dfrac{\xi_{i+1} - \xi_i}{V_{i+1} - V_i}} \tag{42}$$

## EXAMPLE

In this section we consider the experimental data given in Vandermeer et al. (1981) and examine the behavior of a U-Nb alloy with 14.6 at.% Nb. To demonstrate the features of the model we look at the load-temperature histories given in Figure 7 of their paper. The data shown in this figure corresponds to a sample pulled in uniaxial tension from a multiple variant martensitic state to a single variant state and into the plastic range and then unloaded. The unloaded sample is subsequently subjected to a thermal cycle from room temperature to over 1000 K and back to room temperature. To utilize our model the material parameters shown in Table 2 have been found or estimated from the paper.

*REMARK 8:* The choice of material parameters in no way represents optimal values but are merely basic estimates from the reported data. Note that some of the data is taken from a sample with 13.9 at.% Nb and some from a sample with 14.0 at.% Nb.

### Discussion

Shown in Figure 5 is a simulation of Figure 7 from Vandermeer et al. (1981) (compare Figure 6) using load and temperature control.

**Table 2.**

1. Young's Moduli $E_m = E_a = 37.5$ GPa
2. Critical stresses for de-twinning $\sigma^s_{cr} = 150$ MPa and $\sigma^l_{cr} = 325$ MPa
3. Multiple variant martensite temperatures $T_{ms} = 503$ K and $T_{mf} = 318$ K
4. Austenite production temperatures $T_{as} = 325$ K and $T_{af} = 625$ K
5. Austenite production slope $C_a = 0.5$ MPa/K
6. Maximum transformation strain $\varepsilon_L = 0.05$
7. Initial martensite fractions $\xi_0^+ = \xi_0^- = 0.5$
8. Thermal expansion coefficient $\alpha = 20$ $\mu$strain/K
9. Yield stress $\sigma_y = 715$ MPa
10. Hardening modulus $H = 100$ MPa
11. Reference temperature $T = 293$ K
12. Asymptotic austenite fraction $\delta = 0.4$
13. Rate of approach to asymptotic behavior $k = 70$
14. Multilinear break point pairs $(\gamma_1, \beta_1) = (0.1, 0.2)$ and $(\gamma_2, \beta_2) = (0.8, 0.3)$; i.e., tri-linear

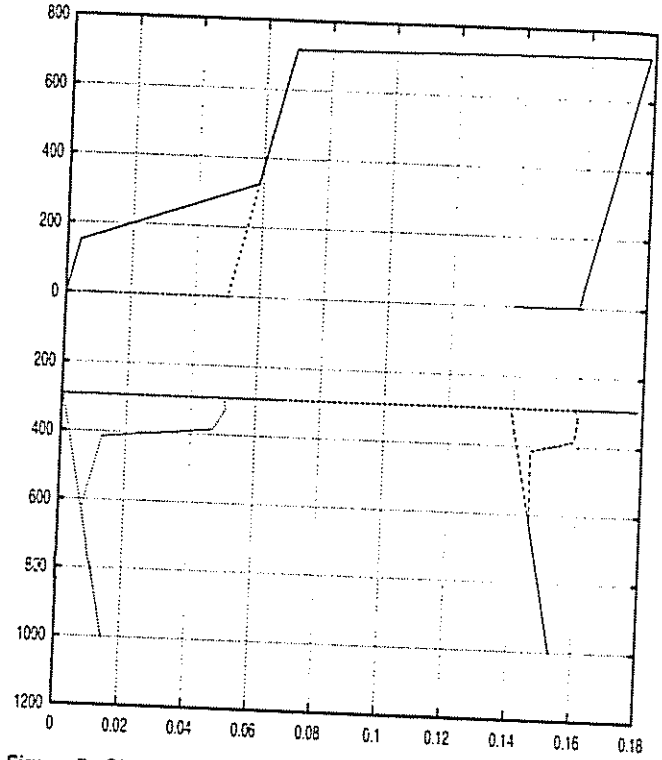


*Figure 5. Simulation of data; stress in MPa versus strain (upper) and temperature in Kelvin versus strain (lower).*

### *STRESS-STRAIN STRAIN-TEMPORARY BEHAVIOR*

A cursory glance at Figures 5 and 6 shows that the proper physics appears to have been incorporated both qualitatively and quantitatively into the model. The material is seen in both the model and the experiment to initially load elastically then begin a martensite de-twinning transformation during an initial plateau followed by an elastic phase and subsequently by plastic deformation. In both cases, when the material is unloaded and subjected to a thermal cycle, we observe a transformation induced recovery of the strain. The recovery strain is seen in both cases to be a function of the total plastic strain to which the material has been subjected.

### *MARTENSITE FRACTION BEHAVIOR*

Shown in Figure 7 is the time history of the plus and minus variants of the martensite fraction for the low strain case and in Figure 8 for the larger strain case.

In both figures we see that there is a production of the positive martensite variant beginning around a time of 3 at the expense of the negative variant. Then around a time of about 21 the de-twinned material begins to transform into austenite. At a time of about 57 the austenite starts to transform back into multiple variant martensite. The effect of the tri-linear transformation curve is easily seen in the production of the austenite. By comparing the two figures we can also see the effect of the plastic strain on the transformation kinetics. Note how at the larger plastic strain, the plus variant of the martensite becomes trapped in the material and is not allowed to transform into austenite as it was able to at

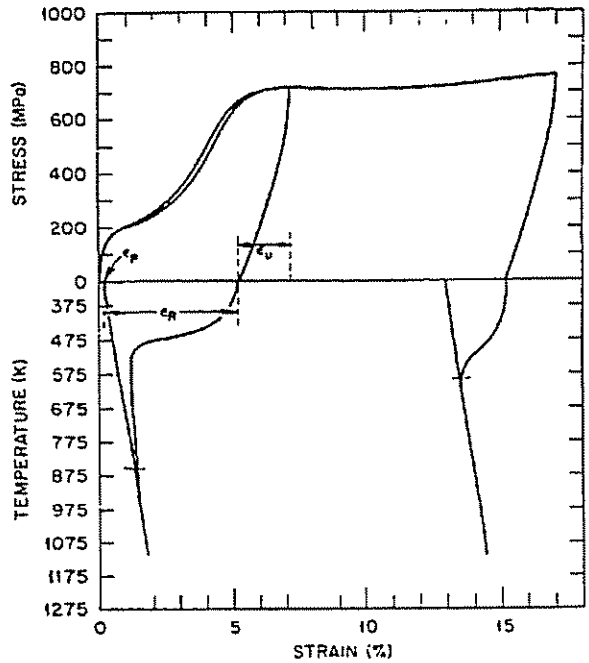


*Figure 6. Strain memory cycle for the uranium + 14.0 at.% niobium alloy initially in the α" state. Upper curve represents the deformation phase, i.e., stress vs. strain while lower curve depicts the thermal response, i.e., strain vs. temperature. Total imparted strains were 7 and 17%. This is scanned data from Figure 7 in Vandermeer et al. (1981).*

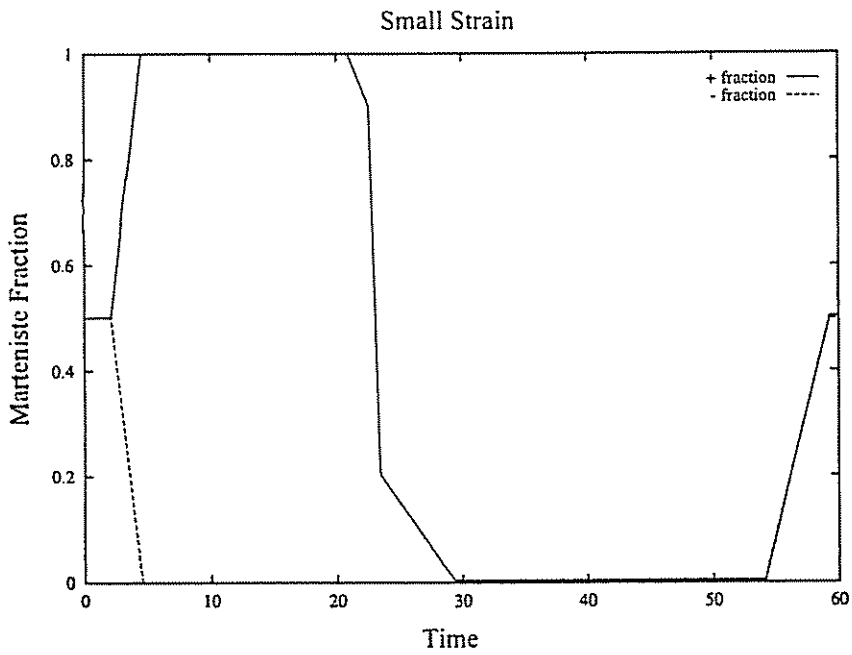


*Figure 7. Predicted variation of martensite fractions with 0.01% plastic strain.*

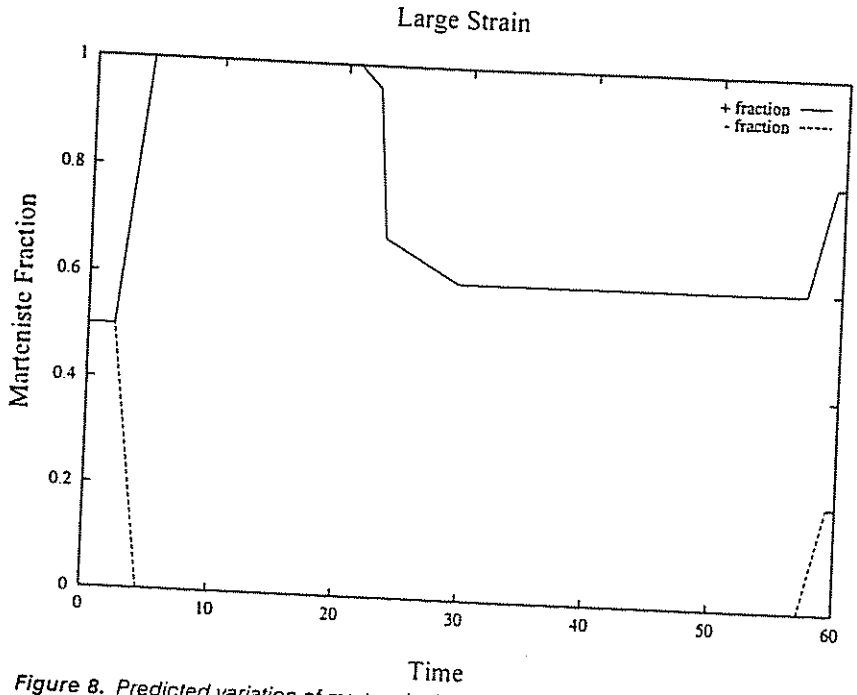


*Figure 8. Predicted variation of martensite fractions with roughly 10% plastic strain.*

the lower plastic strain. The final phase composition of the two experiments are seen to be vastly different in variant fractions.

## CONCLUSIONS

Even though the model provides a qualitatively and quantitatively accurate model, some simple changes are easy to incorporate that will improve agreement with experimental data.

1. The data clearly show that the modulus of the martensitic variants is not the same. Thus one simple improvement would be to set the material modulus to $E = \xi^+ E_m^+ + \xi^- E_m^- + (1-\xi)E_a$. Making this change causes the solution for the martensite fractions during phase transformations to become quadratic and slightly alters the expressions for the algorithmic tangents.
2. Since the available data contained recovery curves at only two levels of strain, one cannot have confidence in the functional form chosen for $f(\bar{\varepsilon}^p)$. Data on recovery curves at intermediate strains will be required to adequately choose an appropriate functional form. Changing this function, however, does not change the theory or algorithm used.
3. The recovery data show a slight dependence of the shape of recovery curve on the amount of plastic strain; i.e., the data shows that the $\gamma_i$'s and $\beta_i$'s are not merely material constants, but rather are functions of $\bar{\varepsilon}^p$. Depending on the accuracy needed in the computations this may be a needed improvement. Changing these parameters to be functions of plastic strain, however, does not change the theory or algorithm used.
4. The model and algorithm presented above do not account for phase transformations that occur in compression. Importantly, the algorithm presented, while attractive for tensile loads with $\xi^- \geq \xi^-$, can fail when the model is naïvely extended to compressive loads when $\xi^- < \xi^-$. The formulation and solution to these more general cases requires the solution of a multi-branch return map; see Kasper (1997) and Govindjee and Kasper (1998).

## REFERENCES

Achenbach, M., "A Model for Memory Alloys in Plane Strain," *Int. J. Solids Structures*, **22**, 171–193 (1986).

Boyd, J. G. and Lagoudas, D. C., "A Thermodynamical Constitutive Model for Shape Memory Materials. 1. The Monolithic Shape Memory Alloy," *Int. J. Plas.*, **12**, 805–842 (1996a).

Boyd, J. G. and Lagoudas, D. C., "A Thermodynamical Constitutive Model for Shape Memory Materials. 2. The SMA Composite Material," *Int. J. Plas.*, **12**, 843–873 (1996b).

Brinson, L. C. and Lammering, R., "Finite Element Analysis of the Behavior of Shape Memory Alloys and Their Applications," *Int. J. Solids Structures*, **30**, 3261–3280 (1993).

Dutkiewicz, J., "Plastic Deformation of CuAlMn Shape-Memory Alloys," *J. Mat. Sci.*, **29**, 6249–6254 (1994).

Ford, D. S. and White, S. R., "Thermomechanical Behavior of 55Ni45Ti Nitinol," *Acta Materialia*, **44**, 2295–2307 (1996).

Govindjee, S. and Kasper, E. P., "Computational Aspects of One-Dimensional Shape Memory Alloy Modeling with Phase Diagrams," *Comp. Meth. Appl. Mech. Engng.*, (in submission) (1998).

Jing-Cheng, W., Zi-Chang, S., Hao, Z. and Hai-Jing, W., "An Anomaly of

the Parameters of Positron Annihilation for Plastically Deforming Shape Memory Alloys," *Scripta Metallurgica et Materialia*, **24**, 1511–1513 (1990).

Funakubo, H. *Shape Memory Alloys*, Translated by: J. B. Kennedy, Gordon and Breach Science Publishers (1984).

Kasper, E., "Shape Memory Materials: Constitutive Modeling and Finite Element Analysis," Ph.D. Dissertation, University of California at Berkeley, Berkeley, CA, Fall 1997.

Pence, T. J., Grummon, D. S., and Ivshin, Y., "A Macroscopic Model for Thermoelastic Hysteresis in Shape-Memory Materials," in *Mechanics of Phase Transformations and Shape Memory Alloys*, AMD-Vol. **189/PVP-Vol. 292**, ASME Press, 45–58 (1994).

Simo, J. C. and Hughes, T. J. R. *Elastoplasticity and Viscoplasticity: Computational Aspects*. Springer-Verlag, (to appear 1998).

Tanaka, K., "A Thermomechanical Sketch of Shape Memory Effect: One-Dimensional Tensile Behavior," *Res. Mech.*, **18**, 251–263 (1986).

Vandermeer, R. A., Ogle, J. C., and Northcutt, W. G., Jr., "A Phenomenological Study of the Shape Memory Effect in Polycrystalline Uranium-Niobium Alloys," *Metallurgical Trans. A*, **12A**, 733–741 (1981).